UC Berkeley
UC Berkeley Previously Published Works

Title

Invited Review Article: Methods for imaging weak-phase objects in electron microscopy

Permalink

Journal

ISSN

Author

Glaeser, Robert M

Publication Date

DOI

Peer reviewed

CrossMark
click for updates

Invited Review Article: Methods for imaging weak-phase objects in electron microscopy

Robert M. Glaeser[a)]

Life Sciences Division, Lawrence Berkeley National Laboratory, University of California, Berkeley, California 94720, USA

Contrast has traditionally been produced in electron-microscopy of weak phase objects by simply defocusing the objective lens. There now is renewed interest, however, in using devices that apply a uniform quarter-wave phase shift to the scattered electrons relative to the unscattered beam, or that generate in-focus image contrast in some other way. Renewed activity in making an electron-optical equivalent of the familiar "phase-contrast" light microscope is based in part on the improved possibilities that are now available for device microfabrication. There is also a better understanding that it is important to take full advantage of contrast that can be had at low spatial frequency when imaging large, macromolecular objects. In addition, a number of conceptually new phase-plate designs have been proposed, thus increasing the number of options that are available for development. The advantages, disadvantages, and current status of each of these options is now compared and contrasted. Experimental results that are, indeed, superior to what can be accomplished with defocus-based phase contrast have been obtained recently with two different designs of phase-contrast aperture. Nevertheless, extensive work also has shown that fabrication of such devices is inconsistent, and that their working lifetime is short. The main limitation, in fact, appears to be electrostatic charging of any device that is placed into the electron diffraction pattern. The challenge in fabricating phase plates that are practical to use for routine work in electron microscopy thus may be more in the area of materials science than in the area of electron optics. © *2013 AIP Publishing LLC*. [http://dx.doi.org/10.1063/1.4830355]

I. INTRODUCTION

A. Electron microscopy of unstained, frozen-hydrated macromolecular complexes plays an important role in biochemistry and molecular biology

Imaging unstained biological macromolecules with the electron microscope has become an important technique in structural biology. These thin specimens can be imaged in an electron microscope even though they are essentially transparent to the electron beam. This is because such specimens cause a significant modulation in the phase of the transmitted electron wave, even though they cause an almost negligible amount of spatial modulation in the amplitude.

In order to image macromolecular structures in a close-to-native state, specimens are first prepared in the form of a thin aqueous film. These specimens are then frozen so rapidly that the water vitrifies rather than crystallizes.[1] Such specimens are examined in the vacuum of the electron microscope while held at a temperature below the aqueous glass-to-crystal phase transition temperature. Holding samples at this low temperature also ensures that the sublimation rate of water in the specimen is negligible. The use of frozen-hydrated specimens, often referred to as cryo-electron microscopy (cryo-EM), thus allows one to record images of randomly dispersed, individual ("single") particles, without the need to prepare crystals suitable for X-ray diffraction experiments. Nevertheless, because of the issue of radiation

damage, the electron exposures must remain very low.[2] As a result, data must be merged from large numbers of single-particles in order to achieve sufficient statistical definition of high-resolution details.

As indicated above, the interaction of high-energy electrons with thin, ice-embedded specimens of biological macromolecules is well described by the "weak-phase object" approximation. This means that the wave function for electrons transmitted through the specimen at a point (x, y) is approximated by

$$\Psi_{Exit\,wave}(x, y) = 1 - i\frac{2\pi e}{h v}V'(x, y), \qquad (1)$$

where e is the electron charge, h is Planck's constant, v is the electron velocity, and V' is the line integral of (i.e., two-dimensional projected value of) the electrostatic potential of the atoms making up the specimen. The second term on the right-hand side of Eq. (1) represents a spatial modulation of the phase of the wave function below the specimen, and the magnitude of this modulation is small compared to 1. The Fourier transform of this term, in turn, represents the wave function for the elastically scattered electron wave. A further description of the weak-phase object approximation is given in Chapter 3 of Ref. 3, and factors that can invalidate this approximation are discussed in Chapter 15 of the same book.

In cryo-EM, images are currently recorded under bright-field conditions. As explained below, these bright-field images are intentionally taken out-of-focus in order to generate contrast. While the image intensity for weak

a)Electronic mail: rmglaeser@lbl.gov

phase objects remains linear in the projected electrostatic potential, it nevertheless is convoluted by a point-spread function due to the intentional defocus (for additional detail, see Sec. 3.7 of Ref. 3). As a result of this linear relationship, the phases of the structure factors of the object are retained in the computed Fourier transform of the image intensity. A defocused bright-field image is, in fact, an in-line hologram (similar to the type of hologram first proposed by Gabor[4]) in which the above-mentioned phase modulations in the exit wave are converted into intensity modulations.

One of the recent – and more impressive – accomplishments of single-particle cryo-EM has been to greatly improve the resolution of three-dimensional (3D) density maps obtained by cryo-EM of icosahedral virus particles.[5] The quality of these maps now makes it possible to see, at a resolution between 0.3 and 0.4 nm, density for individual amino acid side chain residues. Such high-resolution maps allow one to build a model of the polypeptide chain at atomic resolution. The 60-fold (or higher) symmetry of icosahedral viruses helps in two ways to make such high resolution possible. First of all, the 60-fold "amplification" in the size of the structure increases the amount of information (signal) that can be used to align particles. In addition, one can take advantage of this structural redundancy (i.e., point-group symmetry) when merging (averaging) data, thus resulting in a corresponding reduction in the number of particles needed in the data set. A similar result has also been achieved with a considerably smaller, 1.2 MDa enzyme complex consisting of 36 identical subunits.[6]

Even more impressive are the results obtained by using a new generation of fast area-detector to record a series of images (i.e., "movies") in which the electron exposure is divided into frames that are computationally aligned before they are added together.[7] Bai *et al.* used this strategy together with a mathematically sophisticated alignment of images of individual ribosome particles (rather than of entire image frames).[8] The resulting density map clearly showed single amino acid side chain residues in well-ordered parts of the structure, something that no previous electron microscopy work on ribosomes had been able to achieve. In addition, Bai *et al.* found that they could now get such high-resolution density maps with only 1-to-2 per cent the number of particles that previous authors have used. Li *et al.* used a similar approach to get images of a much smaller protein machine, the 20S proteasome, at a resolution of 0.33 nm.[9] In this case, since the contrast of the smaller particle was too low, they could not align individual particles. Li *et al.*[9] thus had to rely on aligning larger segments of the images, and they also merged data from many more asymmetric units than did Bai *et al.*[8]

More often, however, it remains the case that 3D density maps are obtained at a resolution that is not yet high enough to see density for individual amino acids. Even these lower-resolution maps already provide valuable information. If structures of one or more subunits of a multi-protein complex are already known from X-ray crystallography, for example, one can make a pseudo-atomic, "hybrid" model by docking the X-ray model into the EM density map. A recent example has been to make an atomic model of the 26 S proteasome, a very complex molecular machine consisting of at least 32 different subunits.[10–12] Finally, even if the resolution

of a map is not yet at the sub-nm level needed to visualize helices, cryo-EM can provide useful information about the location of different subunits relative to one another within the structure. It is becoming common for such EM structures to be deposited in the EMDataBank (http://www.emdatabank.org/), where they are available for retrieval by others. At present there are over 1700 map entries in the EMDB, about one quarter of which are at a resolution better than 1 nm, and another 40% of which range in resolution from 1 nm to 2 nm.

B. The current technical performance of cryo-EM nevertheless falls well short of what physics allows

Although single-particle cryo-EM is now established as a valuable tool in structural biochemistry and molecular biology, the potential exists for considerable further improvement. The ability to obtain high-resolution structures, comparable to those of the icosahedral virus particles, the ribosome particles, or the 20S proteasome particles mentioned above, should theoretically be possible for macromolecules as small as 50 kDa.[13–15] In addition, it still appears necessary to merge (average) data from approximately $\sim 10^5$ individual particles (asymmetric units), even when correcting for beam-induced movement, in order to achieve the signal-to-noise required at a resolution approaching 0.3 nm.

In theory, on the other hand, images of as few as $\sim 10\,000$ particles should be required to obtain structures at high resolution. It thus is clear that there is still a large gap between what currently is achieved by cryo-EM and what physics would allow. In other words, further improvements in instruments and methodology could make cryo-EM be an even more valuable tool than it currently is. One area in which further improvements can be expected is that of monolithic active pixel sensor (MAPS) technology.[16–18] Image contrast is yet another area where current practice falls far short of what physics allows, however, and that is the topic covered by this review.

C. Low-resolution image contrast in defocused images is only a fraction of what physics would allow

The electron-optical performance of electron microscopes is actually close-to-perfect at intermediate and high resolution. In modern electron microscopes, for example, one can get nearly perfect contrast transfer over the frequency band from 1/(1 nm) to 1/(0.3 nm) by using the so-called Scherzer defocus condition (see, for example, chapter 3 in Ref. 3).

Unfortunately, when used in the bright-field mode, electron microscopes produce almost no contrast at low resolution, for (close-to-focus) images of weak-phase objects. For a fully corrected electron microscope, in fact, the in-focus image intensity is almost constant across the field of view. As noted by Zernike[19] (in the context of light microscopy), this fact "has never bothered the practicing microscopist," because bright-field contrast can still be generated by intentionally defocusing the image. As mentioned above, such "defocused images" are in-line holograms, the intensity of which preserves some of the information contained in the phase of the exit wave. Nevertheless, defocusing the image corrupts the

contrast transfer at high spatial frequencies,[20] and it still continues to give poor contrast transfer at low spatial frequencies.

One can improve the image contrast at low spatial frequencies by defocusing much more, in order to see where the particles are located, but this is achieved at the expense of corrupting the contrast transfer at intermediate and high resolution. Alternatively, one might think to record two or more images, the first at Scherzer defocus (to record information at intermediate and high resolution) and the second at a much greater amount of defocus (to locate the particles of interest). While this approach does have potential, it will be even better if a single image can more fully capture the information contained in the phase modulations of the exit wave.

D. Exploring our options for better image contrast

There are, in fact, a large number of alternative ways in which images might be recorded in existing electron microscopes, or in some cases an appropriately modified instrument. As we will see, however, choosing to record images by one or another of these alternatives may involve making certain theoretical and practical compromises. The goal of this review is to critically evaluate the compromises and trade-offs that are associated with different imaging methods, and to indicate which of these methods appear to have the greatest potential for further improvement.

II. ALTERNATIVES TO USING DEFOCUSED BRIGHT-FIELD IMAGES

A. Diffractive imaging

Although much of the information contained in the phase-modulations of the exit wave is lost in the (in-focus) image intensity, in many cases this information is fully retained in the intensity of the Fraunhofer diffraction pattern. It is true that valuable phase information is contained in the diffracted wave, and this information is lost when recording the diffraction intensities. Nevertheless, the continuous nature of the diffraction intensities produced by non-crystalline specimens, for example, can be used to recover the "lost" phase information by an iterative algorithm.[21] This fact provides the basis of a technique called "diffractive imaging."[22] One of the first applications of diffractive imaging with electrons was to determine the helical structure of carbon nanotubes at a resolution of about 0.1 nm.[23]

Diffractive imaging has some very appealing features. The diffraction intensities are insensitive to translational specimen movement (i.e., drift or vibration) and to wavefront distortions such as those caused by lens aberrations or defocus. This fact overcomes two significant barriers that otherwise limit the ability to obtain images at very high resolution.

Another instance in which the phase of the Fourier transform of the scattered wave can be recovered from the diffraction intensities requires that multiple diffraction patterns be recorded in which a confined spot of illumination is moved progressively over the specimen. This technique, referred to as ptychography, thus produces a series of diffraction patterns from partially overlapping areas of the specimen.[24–26] The principle by which phase information remains encoded in the diffraction intensities is easily understood in the case of a crystalline specimen. If the illuminated area is made small enough, the Bragg reflections are broadened out to an extent that they overlap one another. As a result, the overlapping areas of the diffracted beams will interfere with one another constructively and destructively, depending upon their relative phases.

There are, however, a number of uncertainties about whether diffractive imaging (and ptychography) can be successful for cryo-EM specimens. The continuous background intensity of electrons scattered from the vitreous ice cannot easily be subtracted from the continuous scattering produced by the object itself. The presence of this background is certain to interfere with the iterative recovery of phase information in the diffraction pattern of a single macromolecule. Even if one could accurately subtract the expected value of this background, a second issue is the fact that the remaining signal would be very noisy due to the limited electron exposure that one can use with radiation-sensitive biological specimens. It thus seems unlikely that noisy, single-particle electron diffraction patterns could be phased, even though real-space images taken with the same electron exposure can be aligned and merged. The difference between real-space image intensities and (Fourier-space) diffraction intensities is that phase information is retained in the computed Fourier transforms of the former, whereas it must be recovered by applying an iterative algorithm in the latter.

B. Dark-field imaging

Dark-field images are obtained by using only scattered electrons, i.e., the unscattered electrons are excluded when forming an image. In the simplest implementation, the dark-field image intensity corresponds to the local value of total scattering cross-section, i.e., the incoherent sum of all electrons scattered at a given point in the specimen, ignoring the angle at which the electrons were scattered. For a weak-phase object, for example, such an image would correspond to dividing the second term on the right-hand side of Eq. (1) into arbitrarily small regions and measuring the total power in the Fourier transform of each such region. In this way the phase modulation in the exit wave is converted into an intensity modulation at the detector. As a result, the inherent contrast of a given specimen is fully preserved in an in-focus dark-field image.

Arguably the best way to do dark-field imaging is with the scanning transmission electron microscope (STEM). In this instrument the electron beam is focused to a small probe, which is scanned over the specimen in a defined pattern, usually a square raster. For each position of the beam, one measures the total number of scattered electrons, keeping the total number of incident electrons constant. In the simplest implementation, a single detector is used that subtends as large a solid angle as possible, but which excludes the angles subtended by the unscattered electrons.

A disadvantage of dark-field images that are recorded with the STEM is that the fraction of scattered electrons that can be collected decreases as one increases the resolution of the image, i.e., as one focuses the incident beam to a smaller and smaller probe. The reason is that the unscattered electrons diverge from the point of focus with the same angle by which the incident beam had converged when it was being focused. As a result, the detector that is used to measure the scattered electrons must exclude a larger and larger angular region as the size of the focused probe is decreased.

In order to keep the background intensity as small as possible, the dark-field approach is best suited for objects supported by a very thin film. In cryo-EM specimens, however, it is difficult to avoid that there is vitreous ice above and below the macromolecule, as well as all around it. [Removing all of the water by sublimation (i.e., freeze-drying the sample), a technique often used to prepare specimens for dark-field STEM, in not effective in preserving high-resolution structural details.[27]] For optimal specimen preparations, therefore, the background intensity in dark-field images is quite high. In addition, the contrast is matched to a large degree because the specimen is embedded in water (as is also true for bright-field images).

The dark-field mode thus seems to be an unpromising approach for cryo-EM, in spite of having the advantage that it does not rely on defocusing the image in order to produce contrast. There are, in fact, no examples in which dark-field images have been used to obtain high-resolution cryo-EM images comparable to those obtained by bright-field imaging.

C. Off-axis holography

Off-axis holography would seem to be an excellent way in which to record images of weak phase objects. In order to produce an off-axis hologram in an electron microscope, an electrostatic biprism is used to superimpose a reference wave, obtained from an empty area adjacent to the specimen, and a magnified version of the (in-focus) exit wave transmitted through the specimen. Intensity fringes formed by the constructive and destructive interference of these two wave fronts thus encode the phase information that is present in the exit wave.

Considerable effort has, in fact, been invested in using off-axis holography in the context of cryo-EM, but the images have been limited to quite low resolution.[28] The reason for this disappointing outcome is not certain. One plausible explanation is that electrostatic charging of the ice-embedded specimen may fluctuate in response to random specimen-ionization events occurring during the exposure. The resulting temporal fluctuations in the electrostatic potential will be reflected in corresponding temporal fluctuations in the phase of the exit wave.

Indeed, such fluctuations in the phase of the exit wave are believed to be the cause of the so-called "bee swarm effect" that one can see in highly defocused, low-magnification images.[29] Local fluctuations in the phase of the exit wave may thus cause the positions of interference fringes to fluctuate in an off-axis hologram, limiting the resolution at which phase information can be recovered. In on-axis holography (i.e., intentionally defocused bright-field images), on the other hand, these electrostatic fluctuations affect the phase of the unscattered "reference wave" and the scattered wave equally. In effect, "all boats rise and fall with the same tide."

Other factors also make off-axis holography of cryo-EM specimens rather impractical. Foremost among these, the requirement to have a well-characterized reference wave means that the area adjacent to the specimen must be completely empty – indeed, it preferably should not even include vitreous ice. In addition, the field of view over which high-quality interference fringes is produced is limited to an area less than hundreds of nanometers in diameter by the transverse coherence of the incident beam.[30]

D. Thin-film quarter-wave phase plates

Working in the context of light microscopy, Zernike realized in 1942 that selectively applying a 90° phase shift to the unscattered beam can be accomplished by placing an appropriately shaped quarter-wave plate in the back focal plane of the objective lens.[19] Soon thereafter, Boersch proposed to use a thin carbon film as a Zernike phase plate in the electron microscope.[31] The concept was that the average value of the electrostatic potential (shielded potential of the nuclei) of the atoms making up the carbon film, known as the "inner potential" of the film, would cause a phase shift for electrons that pass through it. The details of implementing such a ("Zernike") phase plate in the electron microscope are different from those normally used in the light microscope, however. In the electron microscope, a hole is provided for the unscattered beam, and the scattered electrons go through the carbon-film phase plate. In the light microscope, on the other hand, it is the unscattered beam that goes through the quarter-wave plate.

In the 60+ years following publication of Boersch's initial proposal, a number of unsuccessful attempts were made by various research groups to implement a thin-film phase plate. Since the results were invariably unsatisfactory, few papers were published from work done during this period.[32, 33] Nevertheless, during the course of that work it was recognized that contamination of the phase plates was a significant problem, i.e., radiation-induced polymerization of organic molecules rapidly produces a non-conducting deposit on the phase plate. Charging of this non-conducting deposit then adds an uncontrolled phase shift. Another reason why the early experimental results were so poor might have been that the hole in the carbon film was not small enough. It is now recognized how important it is to apply a phase shift to electrons scattered at very low angle, in order to provide contrast for the low-resolution features in the specimen.[34, 35] On the other hand, it is not true – as once was thought to be the case – that such phase plates failed to perform as desired because of additional elastic and inelastic scattering of the electrons that passed through the carbon film. As pointed out by Danev *et al.*,[34] this latter effect causes only an 11% reduction in the phase-contrast signal relative to what it would be in an ideal case.
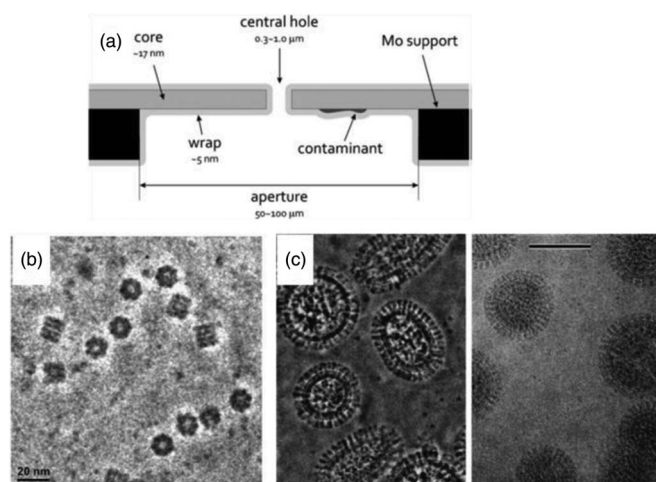
FIG. 1. Schematic diagram of the structure of the thin-carbon-film phase plate, and some representative examples of images that have been obtained with such a device. (a) Cartoon showing one implementation of this type of phase plate. A carbon film (typically <20 nm thick) is supported on a molybdenum aperture, and a focused ion-beam tool is used to drill a hole though the carbon film, at the center of the aperture. This "core" structure is then coated conformally with a second carbon film, which is about 5 nm thick. The purpose of the coating is to cover up any contaminants that may have been deposited in the earlier steps of fabrication. Reproduced by permission from R. Danev, R. M. Glaeser, and K. Nagayama, Ultramicroscopy **109**, 312 (2009). Copyright 2009 Elsevier. (b) Example of cryo-EM images of unstained GroEL, showing the extraordinary amount of contrast that is produced in in-focus images. Reproduced with permission from R. Danev and K. Nagayama, J. Struct. Biol. **161**, 211 (2008). Copyright 2008 Elsevier. (c) A second example of the remarkable amount of contrast that is produced in in-focus images of cryo-EM samples, this time of ice-embedded influenza virus particles. Reproduced with permission from M. Yamaguchi, R. Danev, K. Nishiyama, K. Sugawara, and K. Nagayama, J. Struct. Biol. **162**, 271 (2008). Copyright 2008 Elsevier.

In 2001 yet another such attempt to use thin carbon films as a Zernike phase plate, this time undertaken by Danev and Nagayama,[36] finally succeeded to get promising results. An important innovation in this work was to use a focused-ion beam to mill a small hole in the carbon film (Figure 1(a)), and to also use a large-gap objective lens with a focal length of 3.5 mm. As a result, the cut-on frequency at which phase contrast first began was ∼1/(13.7 nm) for 300 keV electrons. It was again recognized that contamination (radiation-induced polymerization of organic molecules) was still a problem, and thus in subsequent work the phase plate was heated during use.[37] Further improvements included (1) the phase plate was "wrapped" in an additional ∼5 nm coating of evaporated carbon just before use, in order to cover contamination that might have been left after fabrication; (2) the hole diameter was reduced to as small as 0.5 μm; (3) the objective-lens focal length was increased to 5 mm; and (4) the standard objective aperture (which was no longer in the back focal plane of the objective lens) was used as a heat shield to protect cryo-specimens from the heated phase plate.

The experimental results now obtained with the thin-film phase plate are quite good. As the examples in Figures 1(b) and 1(c) illustrate, in-focus phase-contrast images of GroEL (a chaperonin)[38] and of influenza-virus particles[39] show dramatic contrast. Even small protein complexes, such as the 200 kDa dissimilatory sulfite reductase and the 88 kDa

VacA toxin from *Helicobacter pylori*, show quite substantial contrast.[34] In addition, the resolution of phase-contrast images has been shown to be at least 0.8 nm,[40] a value that probably was limited by the CCD camera used rather than by anything to do with the phase plate. Other results are reviewed in Refs. 41 and 42.

Significant improvement is nevertheless needed before the thin-film phase plates can be used for routine cryo-EM applications. The challenge that still remains is that the thin-film phase plates often do not perform well, even immediately after they have been fabricated, and the lifetime of those that initially do perform well may be only a few days. A key signature that performance is failing is that specimens begin to look similar to those in highly over-focused bright field images. At this point one or more oscillations in the CTF also appear at very low resolution.[43] Electrostatic charging of the phase plate is clearly involved, even though the phase plate is heated in order to prevent the buildup of carbonaceous contamination.

Phenomenologically, the thin carbon film thus appears to become more sensitive to radiation damage as it ages. One possible mechanism for charging is that structural changes occur in the irradiated area of the phase plate, and these changes are accompanied by changes in the work function (i.e., local differences in the energy required to remove an electron from the bulk to vacuum) or changes in the contact potential. As a result, radiation damage might result in a local patch where the electrostatic equi-potential surface, outside the carbon film, no longer conforms to the physical surface of the phase plate. While it is plausible that knock-on damage could produce the sort of structural damage envisioned here, it seems puzzling that the sensitivity to such knock-on damage would change with time, i.e., that the carbon film "ages." The cause of charging of carbon films thus is not yet understood, and, in particular, the cause of aging remains a mystery.

E. Electrostatic phase plates

In electron optics, electrostatic potential plays a role for electron waves similar to that of refractive index for light.[44] Electrons are slowed down upon entering a region of negative electrostatic potential, for example, thus increasing their wavelength. As a result, the phase change per length of distance traveled is reduced. A positive electrostatic potential has the opposite effect, of course. [Note, however, that the wavelength of light gets shorter when the speed of light decreases, i.e., when light enters a region where the refractive index is >1.] It thus is natural to think of ways to employ localized differences in electrostatic potential to apply a 90° phase shift to the unscattered electrons relative to the scattered electrons.

1. Self-charging phase plates

One of the earliest attempts to make an electrostatic phase plate was based on the localized electrostatic charging of an ∼0.3 μm diameter fiber of spider silk that was placed in the back focal plane of the objective lens of an electron microscope.[45] The fiber was coated with gold to limit the charging that occurred when irradiated by electrons. Even

though coated with metal, the fiber still became charged when hit by the focused beam of unscattered electrons, presumably because a spot of polymerized contamination was formed, which in turn became positively charged due to the escape of secondary electrons. Although the first published results were of great interest,[45–47] the charging of such fibers proved to be difficult to control, and work with this type of phase plate did not continue.

More recently, the idea of using the focused, unscattered-electron beam to create a localized spot of charging has been taken up again by Malac et al.[48] These authors inserted a continuous (i.e., hole-free) carbon film (or, alternatively, a gold film) into the plane of the electron diffraction pattern. Although the image contrast changes initially with time as the charging builds up, the contrast soon reaches a condition that is stable for a period of time, after which the continuous film may eventually need to be moved to a new location.

It is possible that multiple mechanisms are involved in the charging observed with both the gold-coated fiber and the continuous carbon (or gold) films. (1) Creation of a patch of contamination, mentioned above, is often assumed to be the cause of charging of every type of aperture or phase plate device. In a "clean" microscope vacuum, like that described by Malac et al., this mechanism of charging may limit the length of time over which the aperture can be used, but it is unlikely to be the cause of the initial charging. (2) As an alternative, Malac et al. propose that unspecified, pre-existing "surface layers" become charged. (3) Another mechanism may be involved, however, in the initial (fast) build-up of charge. One suggestion is that knock-on damage to the structure of the thin film is involved, as was mentioned above, or that radiation-induced reconstruction of the surface occurs. Either effect could be accompanied by a change in the work function and the contact potential of the damaged material.

Self-charging of electrically conducting devices that may be covered by an insulating layer (e.g., an oxide layer), or that may develop a spot of contamination on the surface, cannot consist of a localized, net charge, as many assume to be the case. Rather, the charging of such devices must consist of a locally compensated charge distribution. The resulting charge distribution can be represented as a surface dipole layer.[48,49] It thus is important to appreciate how the phase shift produced by an electrostatic dipole depends upon the orientation of the dipole relative to the path of the electron.

There will actually be no phase shift if a dipole is parallel to the electron beam, since the positive and negative charges of the dipole produce equal but opposite phase shifts. If the dipole is perpendicular to the electron beam, however, the electron will experience a distance-dependent phase shift because the impact parameter for the positive charge differs from that for the negative charge by the separation of the two. In the real case, however, even a dipole that is parallel to the electron beam may cause a phase shift if the grounded surfaces surrounding the dipole are not located in a symmetrical way, in which case the actual distribution of electrostatic potential will differ from that of an ideal (free) dipole.

A major disadvantage of self-charging devices is that there is no physical or mathematical (analytical) understanding of the amount of phase shift that they produce. There

is little hope, for example, that such devices could give a constant phase shift over a broad band-pass, and thus a CTF with no oscillations. A constant phase shift is not strictly necessary, however, as long as a device makes it no longer necessary to defocus the image by a large amount in order to see the objects of interest. Image restoration (e.g., phase flipping) can still be based on observable Thon rings, even though their radial position and focus dependence may no longer have a known theoretical dependence on spatial frequency. On the other hand, the goal of using a phase plate is not only to increase the image contrast but also to reduce (not increase) the systematic corrections that have to be applied to images. Furthermore, it seems unlikely that the effect of such a phase plate would be quantitatively stable during the course of a data-collection session, let alone from one session to another. As a result, as will be emphasized below, self-charging is to be regarded as corrupting, not enhancing, the performance of the devices that are currently being investigated. In other words, self-charging is something to be avoided rather than something that can be regarded as producing a useful result.

2. Einzel lens

An einzel lens consists of a stack of three planar electrodes, the middle one of which is biased while the outer two are grounded. Each of the three electrodes has a similarly sized hole, and the three holes are centered about a common axis. Use of a miniature einzel lens as a Zernike phase plate was first proposed by Boersch, in the same paper in which he also proposed the use of a thin carbon film as another type of phase plate.[31] The unscattered beam, which passes through the aligned holes of the einzel lens, feels the electrostatic potential of the biased electrode and experiences a corresponding phase shift. The scattered electrons, on the other hand, pass outside the lens, and thus experience no phase shift. Nevertheless, since electrons that are scattered at very small angle will still hit the electrodes, they are lost and do not contribute to the image. As a result, it is necessary for the dimensions of the entire einzel lens to be small compared to the size of the electron diffraction pattern. Fabrication of a practical einzel-lens phase plate thus requires the use of modern microfabrication tools.

Fabrication of such a miniature einzel lens, suitable for use as a phase plate in electron microscopy, was first reported by Schultheiss et al.[50] As is shown in Figure 2(a), their design included three symmetrically arranged supporting beams, which ensured maximum mechanical stability yet allowed the scattered electrons to still contribute to image formation at the spatial frequencies complementary to those blocked by the supporting structure. Others have subsequently fabricated a similar design with even smaller dimensions.[51–53] A particularly simple version of the einzel lens has been described by Tamaki et al., in which a different metal is used for the central electrode than for the outer electrodes.[54] This version is thus self-biased by the contact potential between the two metals. Another design is also under development, featuring only two symmetrically opposed support beams.[55]
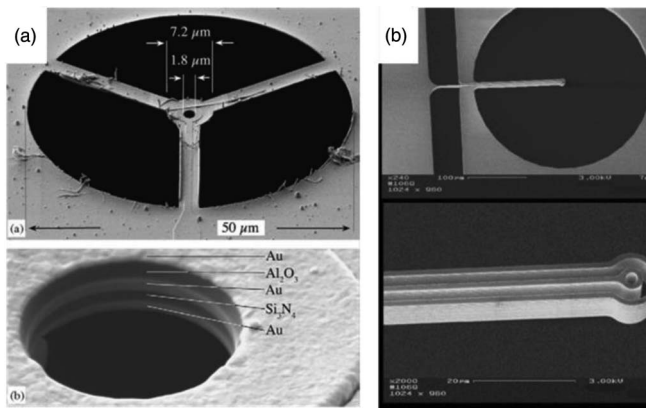
FIG. 2. Two examples of designs that have been proposed for electrostatic phase plates. (a) Scanning electron microscope (SEM) image showing one design for an einzel lens phase plate, which in this case is supported at the center of the aperture by three beams extending from the rim of the aperture. The inset shows a close-up view of the central hole of the einzel lens, revealing the two layers of insulating material that separate the grounded layers of gold, top and bottom, from the biased layer of gold at the center of the device. Reproduced with permission from E. Majorovits, B. Barton, K. Schultheiss, F. Perez-Willard, D. Gerthsen, and R. R. Schroder, Ultramicroscopy **107**, 213 (2007). Copyright 2007 Elsevier.[84] (b) SEM image of the drift tube design of an electrostatic phase plate. The top panel shows an overall view of the aperture, and the lower panel shows a close-up view of the central, biased electrode surrounded by a grounded electrode. The focused, unscattered electron beam passes through the center of the biased tube, and thus experiences a phase shift relative to the scattered electrons, which pass outside the grounded electrode. Reproduced with permission from R. Cambie, K. H. Downing, D. Typke, R. M. Glaeser, and J. Jin, Ultramicroscopy **107**, 329 (2007). Copyright 2007 Elsevier.

If inserted directly into the back focal plane of the objective lens, the dimensions of all such devices are still too large for typical biological applications, where a cut-on frequency of at least 1/(40 nm) is desired.[34] To achieve such a low cut-on it thus is necessary to insert these devices at a plane where the electron diffraction pattern has been magnified.[52]

A major advantage of the einzel-lens phase plate (except for the contact-potential version) is that the amount of phase shift can be tuned to any desired value by adjusting the bias voltage that is applied to the central electrode. The ability to adjust the amount of phase contrast may be important for biological macromolecules 20 nm or more in diameter, for which the contrast produced with a quarter-wave phase plate begins to be large enough to show noticeable departures from a linear dependence on the projected Coulomb potential.[34] In such cases, adjusting the amount of phase shift to less than 90 degrees can result in images for which the intensity of different features more closely approximates a projection of the structure. Possibly even more important will be to reduce the strength of phase contrast when doing cryo-EM tomography, where much thicker specimens are usually used, and these are certain to be very strong phase objects.

Electrostatic charging of the einzel lens is the major technical problem that still must be overcome in order to use it in routine biological, cryo-EM applications.[53] The electrostatic potential associated with charging of the device can cause additional phase shifts that were not intended in the design of the phase plate. When an amorphous carbon film is used as a test specimen, these additional phase shifts may be responsible for distorting the shape of the Thon rings, i.e., the maxima and minima in the Fourier transform of the images. Even when the stigmator is adjusted to make the Thon rings as circular as possible, the radial position of maxima and minima may not be accurately described by the known effects of defocus and spherical aberration. Since there is no physical model of the cause (source) of charging, one cannot deal with it simply by applying a systematic correction, similar to what is done to correct for the contrast transfer function (CTF) in defocused bright-field images. Heating the device to a temperature of 120 °C during use reduces the amount of charging, but this does not fully eliminate the problem.[53]

3. Drift tube

Another design of electrostatic phase plate can be described as a biased drift tube surrounded by a grounded guard electrode. Proof-of-concept experiments along with a recipe for device fabrication were published by Cambie et al.[56] An example of what such devices look like is shown in Figure 2(b). The advantages of this design relative to the enzel lens are that it is relatively easily fabricated from doped silicon, using techniques for high aspect-ratio lithography. The electrodes are separated by vacuum rather than an insulating layer, thus eliminating one of the possible causes for electrostatic charging and radiation damage. In addition, the fringing field can be reduced to a rather small level by fabricating devices in which the length of the tube is ∼10 times the width of the walls and trenches.

Other features of the drift-tube design are similar to those of the einzel lens. The sizes are similar, and thus it is again important to magnify the electron diffraction pattern at the plane where the phase plate is inserted, in order to achieve a lower cut-on frequency. Just as for the einzel lens, the amount of phase contrast is tunable. Electrostatic charging represents perhaps the only technical challenge that still prevents this phase plate from being used in practice.

4. Anamorphic device

As is illustrated in Figure 3(a), the anamorphic phase plate looks like a narrow slit with small electrodes placed at the middle. This phase plate again incorporates a biased electrode that is surrounded top and bottom by grounded electrodes, conceptually similar to the einzel lens. The basic concept[57,58] is to insert two such devices within an aberration corrector, at conjugate planes where the multipole optics produce images of the electron diffraction pattern with a substantially different magnification in one direction relative to that of the perpendicular direction. In one implementation, a local electrostatic potential is used in each respective device to apply two successive, 45° phase shifts, first in one direction and then in a direction perpendicular to the first. The final result is to apply a 90° phase shift to the unscattered electrons, while applying little or no phase shift to the scattered electrons.

This design is very elegant, but in practice there may be formidable challenges. Although this design is free of physical obstructions that are placed into the electron diffraction pattern, every point in the electron diffraction pattern is close
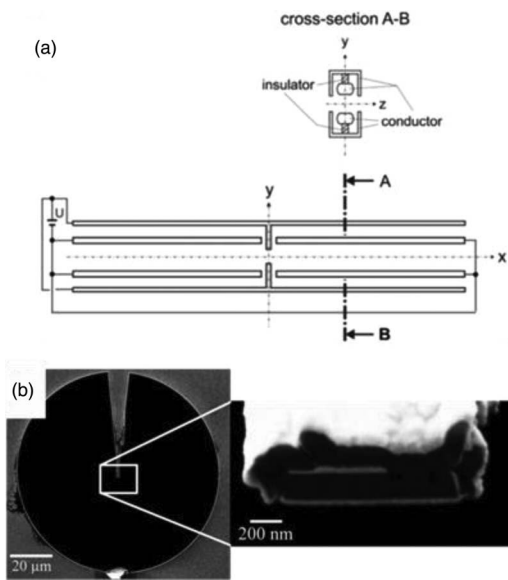
FIG. 3. Images that illustrate the design of the anamorphic phase plate and the (somewhat) related Zach phase plate. (a) Conceptual drawing of the anamorphic phase plate. The electrons propagate parallel to the z axis, and the unscattered beam in the electron diffraction pattern is focused at the intersection of the x and y axes. Furthermore, the diffraction pattern is greatly magnified in the x-direction while at the same time it is greatly demagnified in the y-direction. The biased electrodes produce a localized electrostatic potential that is different at the center of the diffraction pattern than what it is elsewhere. Reproduced with permission from H. Rose, Ultramicroscopy **110**, 488 (2010). Copyright 2010 Elsevier. (b) SEM image of a Zach phase plate, which is a layered beam that extends from the rim to the center of the aperture. The tip of the beam is thus placed close to the center of the electron diffraction pattern. The close-up view on the right shows the biased electrode is exposed at the center of the tip, with a layer of insulation separating it from the surrounding, grounded electrode. This panel is a modified version of a figure published in Ref. 59.

to an edge of the aperture, and thus electrostatic charging of surfaces is again an issue. Alignment of the two, separate phase-plate elements will be difficult if it proves to be necessary to avoid hitting the edges of the slit-like apertures with the electron beam during setup. Finally, in the ideal case, one wants the electrostatic potential to be homogenous across the gap, and, in addition, one wants the fringing field to fall off rapidly from the middle, along the direction of the slit. The extent to which either of these conditions can be met has not yet been established.

5. Zach device

The Zach phase plate,[59] the design of which is shown in Figure 3(b), is similar to one of the electrodes of an anamorphic phase plate, for which it could be considered to be a prototype. This device is meant to be inserted into a standard (isotropic magnification) electron diffraction pattern, however.

The Zach phase plate is essentially a narrow, multilayered beam, the core of which is a biased electrode and the outermost layer of which is a grounded electrode. In this case extensive modeling of the electrostatic potential at the tip has been carried out.[59] Although the applied potential is well localized by making the tip as small as possible, the potential still exhibits a steep gradient close to the open edge of the

beam. It thus is recommended to place the open tip of the electrode a small distance from the center of the diffraction pattern, where the gradient of the potential across the unscattered electron beam will not be too great. This still leaves one with a highly asymmetric phase shift that is applied to the low spatial frequencies in one direction, as well as producing single-sideband contrast at intermediate and high spatial frequencies in the same azimuthal direction. One way to handle these issues would be to simply eliminate these particular spatial frequencies when processing and merging image data.

The contrast transfer function obtained in experiments to date did not show the desired Zernike-type dependence at low spatial frequencies, and the Thon rings were not circular. Similar problems are encountered with other types of phase plate when "self charging" occurs on features placed closed to the unscatteryed electron beam. It thus may be that there are some undesirable similarities between the spectral distribution of phase shifts applied by the Zach phase plate and those introduced by charging artifacts on other devices.

F. Magnetic, Zernike-type phase plates

A phase shift can be applied to the unscattered beam relative to the scattered beams in an electron diffraction pattern by an appropriately configured magnetic vector potential. To accomplish this, the magnetic field, $\vec{B}$, must be confined to a circular ring, in which case the vector potential, $\vec{A}$, consists of closed loops that are concatenated with (i.e., encircle the lines of) the ring-shaped flux of magnetic field, as is shown schematically in Figure 4. As a result, within the plane of the ring-shaped magnetic field, the vector potential points parallel to (or antiparallel to) the axis of the ring on the inside and in the opposite direction on the outside. In practical terms, a
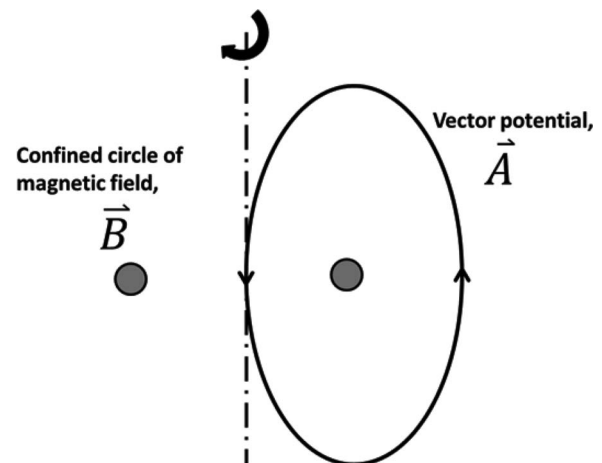

FIG. 4. Schematic diagram showing how the vector field of the magnetic potential, $\vec{A}$, encircles the magnetic field, $\vec{B}$, when the latter is confined to a circular ring. The full, three-dimensional vector field of $\vec{A}$ is generated by rotating the two-dimensional vector field, shown schematically here, about the axis of the ring. The web site http://en.wikipedia.org/wiki/Toroidal_inductors_and_transformers is recommended for a more detailed description. The line integral (i.e., two-dimensional projection) of the vector potential thus has opposite sign for electron rays passing inside the ring and for rays passing outside the ring. As a result, such a structure will produce a relative phase shift for electrons passing inside vs outside the ring.

microfabricated, ring-shaped thin film of ferromagnetic material, rather than a toroidal solenoid, can be used to fabricate such a device on a size scale that is suitable for use in an electron microscope.[60]

The phase shift due to the vector potential was explained by Ehrenberg and Siday in terms of the effect that the vector potential has on the electron-wave surfaces (in semi-classical electron optics),[44] and by Aharonov and Bohm in terms of quantum mechanics.[61] It is often said that this phase shift is a purely quantum mechanical effect without any counterpart in classical physics, because no Lorentz force acts on the electrons. As pointed out by Boyer,[62,63] however, the Lorentz force is not the only classical-physics force that is involved. The moving electron also generates a magnetic field of its own, which in turn interacts transiently with the magnetic field that is confined within the ring. This classical interaction causes a transient change in the electron velocity (hence wavelength), which correctly accounts for the phase shift and provides a classical counterpart to the quantum electrodynamical, Aharonov-Bohm (AB) effect. Interestingly, the magnitude of the phase shift is independent of the electron energy.

The type of magnetic phase plate described here is similar to an einzel-lens device in that both have a central hole through which the focused, unscattered electron beam passes and a narrow, ring-shaped region that obstructs electrons scattered at small angle. In addition, the magnetic device, like the einzel lens, must be supported is some way. Finally, the electrostatic charging that currently is a problem for all such devices will once again have to be overcome. An advantage of the magnetic phase plate is that the phase shift due to the vector potential is the same for all spatial frequencies, provided that there is no leakage of magnetic flux outside the ferromagnetic ring, whereas there will always be some fringing field for the electrostatic phase plate. A shortcoming of the magnetic phase plate is that the amount of phase shift is not easily tuned (changed) during use.

G. Diffractive rather than refractive phase plates

As the heading of this section indicates, it is possible to use local differences in the pattern of a diffraction grating, rather than local differences in the refractive index, to apply a relative phase shift to two different areas of a wave front. In the case of diffraction, the phase shift occurs due to a difference in path length that is followed by one area of the wave front when producing constructive and destructive interference, relative to that for the other area. In the more familiar case of a refractive phase plate, on the other hand, the phase shift is caused by a difference in wave length, and the path length traveled is held constant for both areas of the wave front.

To explain further, imagine that a (one-dimensionally ruled) grating is split into two pieces that remain pressed together, creating a seam that is perpendicular to the lines of the grating. Then imagine that one piece is shifted relative to the other by half the repeat distance, while maintaining contact between the two pieces along the seam. Separate portions of a wave that pass through the two respective sections of the grating will, in the far-field limit, be diffracted to the same point, but when they arrive at that point the phase of one will be shifted by 180° relative to that of the other. Such a "split" grating would thus be suitable for producing Hilbert-contrast images (see Sec. II H 2 for more about Hilbert contrast).

While diffractive phase filters appear to be very interesting for optical microscopy, the efficiency with which electrons can be directed into a given diffraction order is currently relatively low. Since there is no known advantage that would compensate for this loss of electrons, such as insensitivity to charging, this type of mask may be not be useful in cryo-EM applications.

1. Diffractive version of a "Zernike" phase plate

To form a grating that will produce Zernike phase contrast, imagine cutting a small disk out of the middle of a one-dimensional, blazed grating. Then imagine replacing the disk with one that has an identical pattern, but which is shifted by a quarter of the repeat distance. As was pointed out in Figure 2(D) of Furhapter et al.,[64] such a grating can be used to apply a phase shift of 90° to the unscattered beam, by placing the grating in a plane where the Fourier transform of the exit wave is formed. When the unscattered and scattered components of the wave are again combined (i.e., in the in-focus image plane), the result will be a Zernike phase-contrast image, just as if a (refractive) quarter-wave plate had been used to apply the phase shift.

2. Other, quite unusual effects can also be realized

Some rather exotic phase (and amplitude) manipulations can be applied by using diffractive elements. When a Y-shaped edge dislocation is fabricated at the center of a one-dimensional grating, for example, a phase singularity occurs at the core of the dislocation. If such a grating is illuminated by a plane wave, the resulting diffracted beams follow a spiral path,[64] and thus have been aptly called "vortex" beams,[65,66] which are said to carry orbital angular momentum.[65–67] Another example is a grating (diffractive phase mask) in which the phase shift increases as the third power of the distance from the center. In this case the diffracted beams preserve their shape as they propagate, even to the extent that the shape is restored after passing an obstacle.[68]

A number of investigations have been made of the use of a spiral filter in light microscopy. Furhapter et al. demonstrated, for example, that the average light intensity in the image plane is conserved when a spiral (vortex) filter is used, but that the brightness is now concentrated at gradients of the refractive index.[64] Such images are thus similar to Nomarski-contrast images, but the physical mechanism by which the two types of image are produced is quite different. Jesacher et al. have also experimented with several variations of spiral phase elements in which the phase of the central element was varied in order to give a shadowing-like effect, similar to that seen in Hilbert-contrast images or in single-sideband (schlieren) images.[69]

Spiral phase plates have been fabricated on a size scale that can be used with high-energy electrons.[65–68] As was indicated above, however, the poor efficiency with which electrons can be directed into a given diffraction order may prevent this type of phase plate from being useful in cryo-EM applications.

H. Devices that break the Friedel anti-symmetry of the scattered wave

The absence of contrast in in-focus, bright-field images of weak phase objects can be attributed to the Friedel anti-symmetry of the scattered wave function. To explain, the projected Coulomb potential that appears in Eq. (1) is a real-valued function, and thus its Fourier transform is Friedel symmetric, i.e., $F(-\vec{s}) = F^*(\vec{s})$. It is, in fact, the factor of "i" in Eq. (1) that causes the intensity of the in-focus image to be constant (to first order in V'), and that also causes the scattered wave function to be Friedel anti-symmetric. Zernike phase contrast can thus be understood to result from multiplying the scattered wave function by an additional factor of "i," thereby modifying the scattered wave function such that it becomes Friedel symmetric, and at the same time converting phase modulations into amplitude modulations.

At this point one might wonder whether breaking the Friedel anti-symmetry of the scattered wave function in other ways would also create contrast in the image intensity. The answer is yes, it does. Perhaps the easiest way to break the Friedel anti-symmetry of the scattered wave function is to block, i.e., set to zero, part of the electron diffraction pattern with an aperture. If half of the scattered wave is blocked by a "knife edge," the resulting images are said (in the field of electron microscopy) to be single-sideband images.[3] In other fields, use of a knife edge is often called "schlieren optics," as such images reveal the transparent streaks ("schlieren") and other spatial imperfections that occur in glass windows, for example.[70] The basic principle of modifying a half plane of the scattered wave is more general than simply setting it to zero, however, as any modification of the amplitude and/or phase will create contrast in the resulting image intensity of a weak phase object.

1. Half-plane apertures (single-sideband, Foucault, or schlieren contrast)

The use of a knife edge to detect imperfections (phase errors) in a focusing mirror was first reported by Foucault in 1858 (see http://en.wikipedia.org/wiki/Foucault_knife-edge_test). Even today this simple device remains in use as a way to detect wave-front errors caused by imperfections in the "figure" of a mirror.

When a half plane of the scattered wave function is blocked, each Fourier component contributes a term of the form $\cos(2\pi s \cdot x + \alpha(s) + \frac{\pi}{2} - \gamma(s))$ to the image intensity, where s is the spatial frequency of the Fourier component, $\alpha(s)$ is the phase of the Fourier component, and $\gamma(s)$ is the wave aberration (due to defocus and spherical aberration, for example).[3,71] Note that the signal of each Fourier component of the image is 0.5 of what it would be in a Zernike phase-contrast image, because only half of the scattered electrons contribute to the image.

As the expression in the paragraph above shows, there is a systematic phase shift (of each Fourier component) that is equal to ($\frac{\pi}{2} - \gamma(S)$). The systematic, 90° phase shift results in there being an appealing, three-dimensional appearance of features in the image, an effect that has been called "optical shadowing"[72] or "topological contrast."[73] In general, however, it is preferable to use image processing to systematically correct the phases in order to restore the linear relationship between the image intensity and the projection of the Coulomb potential of the specimen.

The Fourier amplitude of a single-sideband image is independent of defocus. This means that the amplitude spectrum does not show the familiar "Thon rings" that are seen in the amplitude spectra of double-sideband images. The absence of Thon rings for single-sideband images is both a good thing and a bad thing. On the one hand, it is good that the contrast transfer function (CTF) for single-sideband images does not oscillate. It is especially good that it remains high (i.e., equal to 0.5) at low spatial frequency rather than going asymptotically to zero as it does for double-sideband images. On the other hand, it is a disadvantage that one no longer has Thon rings that can be used to judge the value of defocus or astigmatism.

It thus is an improvement to use an aperture that blocks a half-plane of scattered electrons at low spatial frequencies, where the double-sideband CTF is very poor, but does not block any scattered electrons at intermediate and high resolution. To approximate this ideal case, Buijsse *et al.* used a FIB to fabricate an aperture with an opaque half circle at the center, supported by a beam extending from the edge of the otherwise open aperture,[71] as can be seen for the example shown in Figure 5. This device is referred to as a "tulip" aperture for short, or more formally as a hybrid double-sideband/single-sideband aperture. In recent developments, it has been found helpful to coat such apertures with evaporated carbon to ensure a uniform electrostatic potential at the surface. It is also helpful to heat the aperture during use, similar to what is done with the thin-film Zernike phase plates, to avoid the build-up of polymerized organic contamination.

It may be an advantage that the design of the tulip is very simple, free of small holes or trenches, and containing no layers of insulating materials. In principle, the aperture can be made of a single material, although in practice it may be necessary to coat the basic aperture conformally with an amorphous, or at least nanocrystalline material. In any case, one has greater freedom in choosing which materials to use to fabricate the aperture, the only requirement being that the aperture is opaque to electrons and does not become electrostatically charged. In addition, the position of this type of aperture can easily be alternated between the "centered" position and a "retracted" position, without the unscattered electron beam touching any part of the device.

The main disadvantage of any type of single-sideband aperture is that the image contrast is only half of what it is for Zernike phase contrast. Furthermore, the amount of contrast is not tunable. Finally, as mentioned above, it is necessary
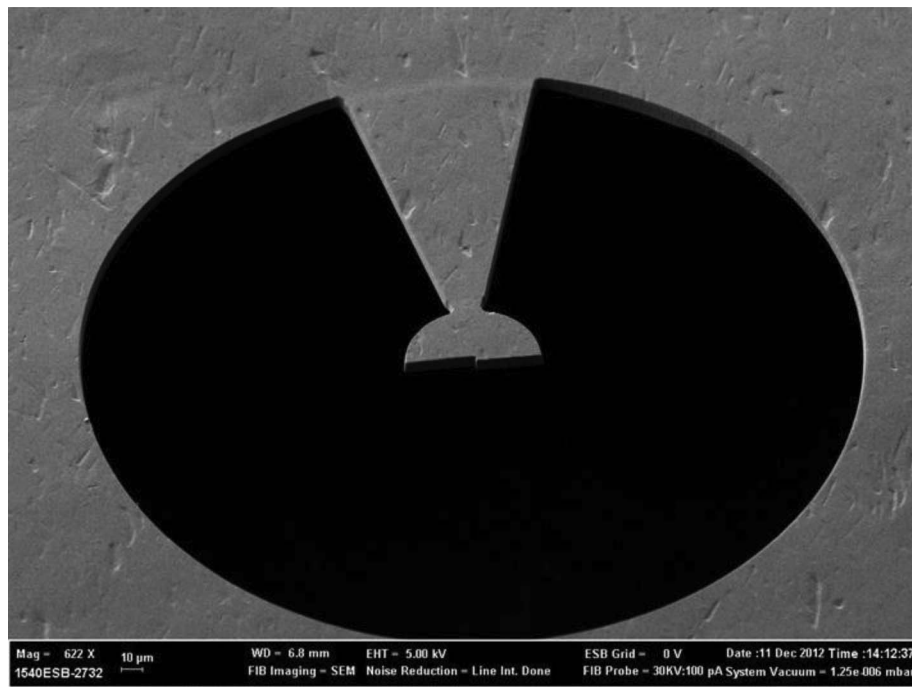
FIG. 5. SEM image of one example of a hybrid double-sideband/single-sideband (tulip) aperture that was made by milling a hole with the desired shape into a thin metal foil, using a focused gallium-ion beam (FIB). The perspective in this image is foreshortened because the aperture was tilted to give an impression of the thickness as well as the shape of the tulip-like feature. The opaque half-circle at the center has a small notch at the center, where the straight edge is off-set from the diameter in one direction on the left, and by the same amount in the opposite direction on the right.

to make a systematic correction of the phases of the Fourier transform of the image, similar to the CTF correction that is needed for bright-field images.

2. 180° phase shift for a half plane achieved with a thin film

A good alternative to blocking a half-plane of the scattered wave function is to apply a 180° phase shift to one half plane relative to the other. This strategy has been said to produce "Hilbert contrast,"[74] which once again gives the impression of a "three-dimensional" nature to the image. Experimental applications of this type of imaging mode include cryo-EM images of intact cells[75,76] and tomographic reconstructions of unstained, resin-embedded cells.[77] In some of these examples, charging of the Hilbert-contrast phase plate may have been present, but this did not prevent getting valid results at low to intermediate resolution. As for single-sideband contrast, one must use post-processing to convert the raw image intensity to one that is proportional to a projection of the structure.

The 180° phase shift required to produce Hilbert contrast was first implemented by using a carbon film that is twice as thick as that which would be used to make a Zernike phase plate. While this is both simple to do and effective, it is also not an ideal solution. One complication is that there now is a significant loss of electrons in one half-plane of the scattered wave front, thus adding a component of single-sideband contrast to the desired Hilbert contrast.

3. Equivalent, 180° phase shift achieved with the Aharonov-Bohm effect

The Aharonov-Bohm effect provides an attractive alternative way to apply a 180° phase shift to one half-plane relative to the other. In this case, a narrow, "infinitely long" bar (rather than a circular ring) of magnetic material is used to confine the magnetic field.[42] Once again, the vector potential encircles the confined magnetic field, thus causing a positive phase shift on one side of the bar and a matching negative phase shift on the other side. By adjusting the width and thickness of the bar, one can produce the desired phase difference of 180° between one half-plane and the other.

As for all other types of phase-contrast apertures, one must take steps to avoid electrostatic patch potentials and other sources of charging. In addition, one must avoid there being any magnetic flux leakage from the (permanent) bar-magnet structure. Unlike the carbon-film type of Hilbert-contrast aperture, there is no partial loss of electrons caused by the magnetic version, other than for the small area blocked by the bar magnet itself. The concept of this type of phase-contrast aperture is sufficiently appealing that further development appears to be worthwhile.

I. Laser (ponderomotive potential) phase plate

In terms of a classical-physics description, it takes work – known as the "average quiver energy" – for an electron to penetrate into a focused spot of light. The electron thus will be first slowed down and then returned again to its original speed as it passes into and then out of an intense spot of

light. As a result, there will be a phase shift for electron paths passing through the region of "ponderomotive potential" that is associated with the focused light beam. The same phase shift can be explained more rigorously in terms of quantum electrodynamics, of course.[78,79]

The laser power that is needed to apply a 90° phase shift to 300 keV electrons is in the range of kilowatts or more, depending upon the wavelength of light and the size of the focused light beam.[78] Reed and colleagues at Lawrence Livermore National Laboratory initially proposed to employ a pulsed laser to achieve the desired power. This requires that the phase plate must be used in conjunction with a synchronously pulsed electron beam (https://ipo.llnl.gov/?q=technologies-phase_plate; US patent number 8,217,352). Another alternative, proposed by Mueller *et al.*,[78] is to focus a moderate-energy, continuous laser beam within a Fabry-Perot cavity, where the circulating power would build up to the required level.

The advantages of the laser phase-plate concept are that the phase shift is tunable, no electrons are lost due to inelastic scattering or absorption, and no mechanical elements are inserted close to the electron diffraction pattern, where they might become electrostatically charged. Working models of such a laser phase plate are still in development, however.

J. Pixelated electron mirrors

Electrostatic electron mirrors, while not commonly used in transmission electron microscopes, nevertheless continue to be used to perform a variety of specialized experiments. In most cases the electrodes that slow down, reflect, and then re-accelerate the electrons are mounted to one side of the main optical axis of the electron microscope. The electron beam is first deflected by 90° (by a magnetic field), and then, after being reflected by the electrostatic mirror, the beam is again deflected by 90° back onto the main optical axis of the microscope. An electron mirror was used, for example, as part of the Henry-Castaing energy-filter lens, which at one time was included in the Zeiss EM902 electron microscope, but which has now been superseded in other instruments by an all-magnetic energy-filter lens.

Okamoto has proposed some conceptually novel ways in which a pixelated electrostatic mirror might be used for improved measurements with radiation-sensitive specimens. In one such device, individual pixels would be created on the mirror surface by microfabrication, with the idea that each could be biased independently relative to the main voltage.[80] Electron rays reflected at different points on the mirror would thus be given a user-defined phase shift. Alternatively, one might also imagine that the surface of the electrostatic mirror could be made with an optically transparent conductor, through which a user-defined pattern of light would be focused at the plane corresponding to the turning point of the electron trajectories. Variations in the intensity of light within this pattern would, in turn, produce a user-specified amount of phase shift at each point.

In the simplest implementation, the electron diffraction pattern would be focused at the surface of the mirror, and only one or a few pixels, corresponding to the unscattered beam, would be biased relative to the main voltage by an amount that would produce a 90° phase shift, thus turning the mirror into a Zernike phase plate. In addition, however, Okamoto proposes much more sophisticated schemes in which the capability of a fully pixelated mirror would be used for adaptive-optics quantum measurements, as these have the potential to significantly reduce the electron dose needed to extract structural information at a given resolution.[80]

In a second development, Okamoto has proposed to reduce the shot-noise at each pixel in the image from the standard quantum limit of $N^{-1/2}$, where N is the number of electrons, to a much smaller value, approaching the value of N^{-1} allowed by the Heisenberg uncertainty principle.[81] To do this, Okamoto proposes to use a Cooper-pair box, integrated within the surface of an electrostatic mirror, to produce a beam of "k" successive electrons, each of which is entangled with the state of the Cooper-pair box, to illuminate the specimen. While the specimen-damage per unit of thickness caused by these electrons is the same as if they were not entangled with the state of the Cooper-pair box, the signal (i.e., the phase modulation referred to the exit wave) would be k times larger than for an image in which the incident electrons are not each entangled with a common reference state. The resulting increase in signal is as if the sample itself were "k" times thicker than it actually is. Because some of the electrons are scattered inelastically, however, it is estimated the beneficial effects of entanglement will be greater for object features that are smaller than ∼1 nm or possibly ∼2 nm, which is the characteristic length for delocalization of the inelastic scattering event. The benefits of entanglement are thus complementary with those of a phase plate, where the greatest benefit is to be gotten at low spatial frequency.

III. CURRENT STATE-OF-THE-ART

Within the past decade a number of improvements have been made in the implementation of in-focus phase-contrast technology. As indicated above, these improvements include heating the phase plate during use (in order to prevent the formation of carbonaceous contamination) and ensuring that the desired phase shift is applied at sufficiently low spatial frequency. In addition, it is now understood, contrary to previous concerns, that electron loss in thin-film phase plates is not a significant limitation. Nevertheless, all types of phase-contrast devices continue to suffer from electrostatic charging, the cause(s) of which are still not understood.

At present, the thin-carbon film (Zernike) phase plate is the only device that has given results in structural biology that go beyond what can be done with defocus-based phase contrast. When this type of phase plate is free of charging, the results fully demonstrate that in-focus phase contrast provides considerable improvement. Protein molecules as small as 88 kDa are readily visible because of the high contrast,[34] as was mentioned above. In addition, an asymmetric reconstruction of the herpes simplex virus capsid revealed the presence of a previously unseen, but expected, "portal complex" on one of the 5-fold symmetry axes.[82]

There have been many other demonstrations that greatly increased contrast is provided by carbon-film phase plates. The one worry about such demonstrations is that dramatic image contrast is also achieved when substantial charging is present. It thus is important to look at the Fourier transform of the image to determine whether the contrast-transfer function (CTF) is indeed what one expects it to be. When a thin-carbon (Zernike) phase plate exhibits charging, as is often the case, the contrast may be similar to that when a "hole-free carbon-film phase plate"[48] is used, where charging is actually the intended source of phase contrast.

By comparison, cryo-EM employing the einzel lens is just beginning to show results, and these still fall short of what can be gotten without a phase plate. Cryo-EM images of tobacco mosaic virus (TMV) have been obtained that show the 2.3 nm layer line,[52,53] and cryo-EM images of "purple membrane" (which is a monolayer crystal of bacteriorhodopsin) extend to a resolution of 0.7 nm or slightly higher.[52] One of the current limitations on the quality of images is the fact that the dimensions of the einzel lens are still too large. As a result, the low-frequency Fourier components of the electron diffraction pattern are blocked, rather than contributing with full phase contrast. In addition, charging of the devices, even when heated to 120 °C, currently produces a contrast-transfer function that cannot be explained by the applied 90° phase shift, the amount of defocus, and the coefficient of spherical aberration.[53]

Cryo-EM employing the tulip aperture also is still at an early stage of development. Nevertheless, as is shown in Figure 6, taken from Ref. 83, high-contrast images have been obtained of monolayer crystals of streptavidin at (or close to) Scherzer defocus. Perhaps the most striking thing is that individual tetramers of streptavidin, whose molecular weight is only 55 kDa, can be seen in the open area between monolayer crystals. Additional documentation has been given to show that completely charging-free operation was achieved when those images were recorded.[83] Nevertheless, it is emphasized that such a charging-free state lasts for only several hours or days of use, and fabrication of charging-free apertures has been inconsistent. In this regard, the situation is quite similar to that of the thin-film phase plate.

For all other phase-contrast devices described above, experimental results – if any – are still limited to images of test specimens such as amorphous carbon film, negatively stained protein samples, or plastic sections of tissue. The objective, at this stage, has been to establish an initial proof of concept, while further developing the method.

IV. SUMMARY AND CONCLUSIONS

A number of new ways to achieve in-focus phase contrast in transmission electron microscopy have been proposed over the past few years, adding to the several options that had been considered previously. A total of 17 physically distinct principles for achieving in-focus contrast (in addition to the currently used, 18th alternative of simply defocusing the image) are identified in Table I. This table includes a few brief statements about the current status of each approach,
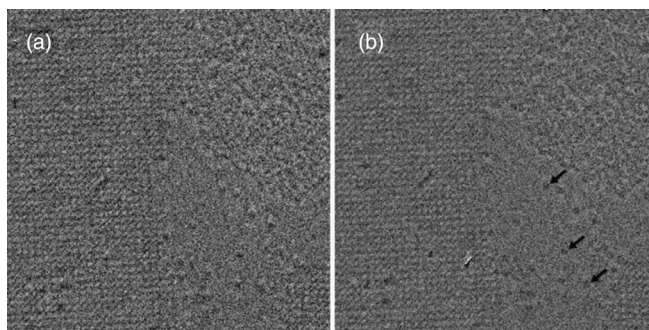

FIG. 6. In-focus cryo-EM image (obtained with a tulip aperture) of an area containing a monolayer crystal of streptavidin. Reproduced with permission from R. M. Glaeser *et al.*, Ultramicroscopy **135**, 6 (2013). Copyright 2013 Elsevier. (a) The raw image shown here exhibits a "shadowed" character due to the single-sideband contrast transfer produced by the tulip aperture. (b) The image shown here is a processed version of the raw image shown in (a), in which a systematic correction has been applied to compensate for the single-sideband contrast transfer. The full amount of contrast provided by this aperture is retained when applying this correction. As a result, individual streptavidin tetramers, examples of which are indicated by the arrows, can be identified quite easily in the non-crystalline area of the specimen, even though their molecular weight is only ∼55 kDa.

and also a few comments on what the key limitations are at present.

Some of these approaches seem more promising than others, based on what we currently know. The various entries are therefore grouped into those that currently seem to be the most promising ones, those that appear to be less promising, and those where it is still too early to tell whether they will be successful or not. In addition, a brief narrative is presented below for each entry, summarizing the relative strengths and weaknesses of each, and repeating what the problems are that need to be solved.

A. The most promising approaches

The Zernike-type **thin-film phase plate** is a strong candidate to ultimately emerge as the preferred design. It has already produced examples of results that could not be achieved just by defocusing the image. The only requirements that remain before the thin-film phase plate can be used routinely for cryo-EM applications are that the fabrication of high-quality devices must be made more consistent, and their working lifetime must be greatly extended. Perhaps materials other than evaporated carbon can be found that will satisfy these requirements. Individual thin-film phase plates do not provide a tunable amount of contrast, of course, but this issue can be overcome to some extent by loading multiple phase plates with different thicknesses, and choosing the one that gives the phase shift that is most suitable for a given specimen.

Alternatively, the **einzel lens** and the **drift tube** (electrostatic) designs may ultimately prove to be the phase-plate solution of choice. The key advantage of electrostatic phase plates is that the amount of phase contrast is tunable. On the other hand, the ability to diminish the amount of phase contrast or to invert its sign is likely to be a significant advantage only for strong phase objects. It may be thought that

TABLE I. Assessment of methods to image weak-phase objects.

	Method	Status	Comments
Current practice	Highly defocused images	This currently remains the best method to image cryo-EM specimens.	Contrast transfer function (CTF) -> 0 at low resolution, even at high defocus.
		Image contrast nevertheless falls far short of what physics would allow	High amount of defocus results in rapid oscillations of the CTF
The most promising approaches	Thin-film "Zernike" phase plate	Numerous excellent results published with cryo-EM specimens.	Reliability and lifetime remain poor (due to charging).
		Commercialized product is available.	Best hope for the future lies with development of better thin-film materials.
	Electrostatic einzel lens ("Zernike") phase plate	Promising cryo-EM results obtained for bacteriorhodopsin crystals and for tobacco mosaic virus.	Reliability and lifetime remain poor (charging).
			Progress is expected to be rapid if causes of charging become known, and can be overcome.
	Electrostatic drift tube ("Zernike") phase plate	Initial proof-of-concept has been shown, but no results for biological specimens.	Progress could be rapid if causes of charging become known and can be overcome.
	Magnetic devices - Ring geometry ("Zernike") - Magnetic bar (Hilbert)	Not yet ready to test with cryo-EM specimens.	Difficult to tune the phase shift. Both devices avoid the issue of fringing fields that occurs for electrostatic devices. Charging is just as problematic as it is for other devices.
	Tulip aperture	Promising cryo-EM results obtained for crystals and for single particles of streptavidin.	Reliability and lifetime remain poor (charging).
Less promising at this time	Thin-film "Hilbert" phase plate	Dramatic contrast shown with biological specimens, including cryo-EM specimens.	Quantitative interpretation of image contrast is complicated due to partial single-sideband contrast.
			Reliability and lifetime are as problematic as for the thin-film Zernike phase plate
	Zach phase plate	No examples of results with cryo-EM specimens.	Steep gradient of electrostatic potential at the tip is not ideal.
			Thon rings do not show "cosine" contrast transfer at low spatial frequency, and show distortion that could not be corrected by stigmation.
	Self-charging fiber	Dramatic contrast shown with biological specimens.	After initial publications the work was not continued, presumably because of unstable charging and inability to model the phase plate.
	Self-charging thin film	Dramatic contrast shown with biological specimens	Modeling the phase plate will be difficult.
	Off-axis holography (biprism)	Cryo-EM results have been obtained; resolution is disappointing.	Specimen charging is much more problematic than for other methods. Limited field-of-view
	Dark-field imaging	No examples of high-resolution results with cryo-EM specimens.	Fraction of incident electrons that are used becomes smaller as the resolution increases.
			Contrast presumed to be small for ice-embedded specimens.
	Diffractive imaging	Impressive results with carbon nanotubes, but little further work beyond that.	Difficult to satisfy the requirement that the object has compact support.
			Signal-to-noise ratio may be inadequate for applications with beam-sensitive specimens.
	Diffractive phase plates	Clever work with light microscopy, but no published work with electrons.	Loss of electrons due to low diffraction efficiency is a serious disadvantage
Devices at too early a stage to evaluate	Laser (pondero-motive) phase plate	Theoretical proposal.	Not yet known what experimental issues might arise in practice.
	Anamorphic (electrostatic)	Theoretical proposal.	Must be used as part of a multipole corrector system.
			Charging issues must be solved, as for the einzel lens.
	Pixelated mirror	Theoretical proposal.	Not yet known what experimental issues might arise in practice.

difficulty in fabricating small enough devices is an issue for electrostatic devices. This is indeed a concern if one hopes to insert an electrostatic phase plate directly in the back focal plane of the objective lens, as a replacement of the standard objective-lens aperture. It is much less of an issue, however, if additional electron optics are used to magnify the electron diffraction pattern by a factor of 5 or 6 at a point further down the column. A further advantage of inserting the phase plate further down the column is that doing so makes it possible to heat the phase plate without risk of warming the cryo-sample.

The loss of information within a band of low spatial frequencies that is blocked by the structure of the electrostatic devices, while an undesirable feature, does not pose a serious problem. The cut-on frequency at which phase contrast first begins can be made as small as 1/(40 nm) (for 300 keV electrons) by a combination of micrometer-scale fabrication and sufficient magnification of the size of the electron diffraction pattern. At least for many applications, the loss of information at even lower frequencies is not a significant factor. The current problem of unwanted electrostatic charging must still be overcome, of course, in order for electrostatic devices to be useful.

The **magnetic ring phase plate** also has potential to become the design of choice. The main advantage of this device is that it can produce a constant spectral-distribution of phase shifts since, unlike the electrostatic (einzel lens and drift tube) phase plates, fringing fields can be eliminated completely. Similarly, the **linear magnetic** (Hilbert) **phase plate** has high potential because the phase shift that it can produce is also free of fringing fields. Up until now, however, both such devices have encountered the same problems of electrostatic charging as have other phase plates.

In the short term, the "tulip-like" version of a **single-sideband aperture** may prove to be a very practical choice for obtaining in-focus images with high contrast. The simple design of this aperture, devoid of insulation between electrodes (like the einzel lens design) or of a high-aspect-ratio central hole and trenches (like the drift-tube design) make the tulip aperture a good choice for experiments aimed at understanding, and ultimately resolving, the issues related to electrostatic charging. Although the tulip aperture cannot provide tunable contrast, and the contrast that it does provide is only half that of a Zernike or Hilbert phase plate, the results are nevertheless expected to be much superior to those obtained by defocusing the image. Furthermore, although image restoration is still required when using the tulip aperture, CTF oscillations, if any, are very slow in the high-resolution part of the Fourier spectrum when images are recorded close to Scherzer defocus.

B. Less promising at this time

The **thin-film Hilbert phase plate** is unlikely to emerge as a preferred choice for applications in cryo-EM. The use of such a phase plate faces the same limitations as does the thin-film Zernike phase plate, and if these limitations can be overcome for the former, then they can also be overcome for the latter. In addition, a more complicated image restoration

scheme is required for quantitative work, since the electron wave function is attenuated in an unsymmetrical way by the Hilbert phase plate.

The **Zach** (electrostatic) **phase plate** also may not be a desirable solution for obtaining in-focus images. As noted above, the electrostatic potential produced by this design has much in common with a small, localized patch of charging that is often seen on other types of apertures. It is true that the magnitude and the location of what is, in effect, a "localized patch potential" is under experimental control for the Zach phase plate. Even so, the spectral distribution of phase shifts is not at as simple as for a Zernike phase plate, or for a Hilbert phase plate.

Self-charging phase plates, such as Unwin's **thin fiber design** or Malac's **hole-free thin film design**, appear to be unsuitable for quantitative work. This is because the user has little control over the amount of charging that occurs and over its stability with time. Furthermore, there is not yet a theoretical description of the spectral distribution of phase shifts that are produced by such devices. These are, in fact, the reasons why (self) charging is so undesirable in the Zernike-type and Hilbert-type of thin-film phase plate.

Off-axis holography, using an electrostatic bi-prism, faces a seemingly insurmountable problem in the fact that fluctuations in specimen charging, rather than charging of the device itself, causes a loss of visibility of interference fringes in the image. Although cryo-EM images have been obtained of tobacco mosaic virus, the results obtained are not as good as those obtained by conventional (defocus based) imaging. In addition, off-axis holography has a small field of view compared to other modes of phase-contrast imaging.

Dark-field imaging has been thought by many as being equal, or even superior to bright-field imaging. While this can indeed be the case if the electron exposure is not a limiting factor, it seems to be a poor choice for cryo-EM. No high-resolution results have been obtained for cryo-EM specimens by dark-field imaging, for example. **Diffractive imaging** is also likely to be unsuccessful for cryo-EM specimens because of the limited electron exposure that can be tolerated. In this case, phasing of the "oversampled," continuous, but noisy diffraction pattern is likely to be unsuccessful. Finally, in the same vein, **diffractive phase plates**, including the versions that use **spiral beams**, are likely to be a poor choice for cryo-EM specimens. In this case, the problem is that only a relatively small fraction of electrons is likely to be diffracted into a single order of the nanofabricated diffraction grating, resulting in a low efficiency of using the electrons to which the specimen was exposed.

C. Devices at too early a stage to evaluate

The **focused-laser (ponderomotive) phase plate** has a number of desirable features. The amount of phase shift is tunable, which is a definite "plus." No physical surfaces are placed close to the diffraction pattern, so electrostatic charging is not expected to be an issue. In addition there are no electron losses due to portions of the diffraction pattern being blocked, or due to scattering during transmission of the

electrons through the phase plate. Indeed, if the problem of charging is not overcome for any of the other devices mentioned above, the most promising device that still remains may well be the focused-laser phase plate.

The **anamorphic phase plate**, in spite of the superficial similarity of the design of its electrodes to those used in the Zach phase plate, may nevertheless produce a more constant distribution of phase shifts. The reasons to think that this may be the case are the more symmetrical design and the apposition of extended, grounded surfaces close to the biased electrode. Quantitative numerical simulations are still needed, however, to establish how much improved the spectral distribution of phase shifts is for the anamorphic phase plate.

The proposed use of a **pixilated mirror** is extremely interesting for a number of reasons. The same device can be used simultaneously as an aberration corrector and a phase plate, for example. In addition, it has been proposed that such a device can be used for experiments in which adaptive optical changes could be an advantage, or for experiments in which the electrons that are used to image the specimen are first entangled with a Cooper-pair box that is integrated into the surface of the mirror.

[1] K. H. Taylor and R. M. Glaeser, J. Struct. Biol. **163**, 214 (2008).
[2] L. A. Baker, E. A. Smith, S. A. Bueler, and J. L. Rubinstein, J. Struct. Biol. **169**, 431 (2010).
[3] R. M. Glaeser, K. Downing, D. DeRosier, W. Chiu, and J. Frank, *Electron Crystallography of Biological Macromolecules* (Oxford University Press, 2007).
[4] D. Gabor, Nature (London) **161**, 777 (1948).
[5] N. Grigorieff and S. C. Harrison, Curr. Opin. Struct. Biol. **21**, 265 (2011).
[6] D. J. Mills, S. Vitt, M. Strauss, S. Shima, and J. Vonck, eLife **2**, e00218 (2013).
[7] M. G. Campbell *et al.*, Structure **20**, 1823 (2012).
[8] X.-c. Bai, I. S. Fernandez, G. McMullan, and S. H. Scheres, eLife **2**, e00461 (2013).
[9] X. Li, P. Mooney, S. Zheng, C. R. Booth, M. B. Braunfeld, S. Gubbens, D. A. Agard, and Y. Cheng, Nat. Methods **10**, 584 (2013).
[10] G. C. Lander, E. Estrin, M. E. Matyskiela, C. Bashore, E. Nogales, and A. Martin, Nature (London) **482**, 186 (2012).
[11] F. Beck *et al.*, Proc. Natl. Acad. Sci. U.S.A. **109**, 14870 (2012).
[12] P. C. A. da Fonseca, J. He, and E. P. Morris, Mol. Cell. **46**, 54 (2012).
[13] R. Henderson, Q. Rev. Biophys. **28**, 171 (1995).
[14] R. M. Glaeser, J. Struct. Biol. **128**, 3 (1999).
[15] P. B. Rosenthal and R. Henderson, J. Mol. Biol. **333**, 721 (2003).
[16] N. Guerrini, R. Turchetta, G. Van Hoften, R. Henderson, G. McMullan, and A. R. Faruqi, J. Instrum. **6**, C03003 (2011).
[17] A. C. Milazzo *et al.*, J. Struct. Biol. **176**, 404 (2011).
[18] M. Battaglia, D. Contarato, P. Denes, D. Doering, T. Duden, B. Krieger, P. Giubilato, D. Gnani, and V. Radmilovic, Nucl. Instrum. Methods Phys. Res. A **622**, 669 (2010).
[19] F. Zernike, Science **121**, 345 (1955).
[20] K. H. Downing and R. M. Glaeser, Ultramicroscopy **108**, 921 (2008).
[21] J. R. Fienup, Appl. Opt. **21**, 2758 (1982).
[22] J. C. H. Spence, U. Weierstall, and H. N. Chapman, Rep. Prog. Phys. **75**, 102601 (2012).
[23] J. M. Zuo, I. Vartanyants, M. Gao, R. Zhang, and L. A. Nagahara, Science **300**, 1419 (2003).
[24] J. M. Cowley, J. Electron Microsc. **45**, 3 (1996).
[25] W. Hoppe, Ultramicroscopy **10**, 187 (1982).
[26] J. M. Rodenburg, in *Advances in Imaging and Electron Physics*, edited by P. W. Hawkes (Elsevier, 2008), Vol. 150, p. 87.
[27] J. Lepault, F. P. Booy, and J. Dubochet, J. Microsc. (Oxford) **129**, 89 (1983).
[28] P. Simon, H. Lichte, P. Formanek, M. Lehmann, R. Huhle, W. Carrillo-Cabrera, A. Harscher, and H. Ehrlich, Micron **39**, 229 (2008).
[29] G. H. Curtis and R. P. Ferrier, J. Phys. D **2**, 1035 (1969).
[30] J. Sickmann, P. Formanek, M. Linck, U. Muehle, and H. Lichte, Ultramicroscopy **111**, 290 (2011).
[31] H. Boersch, Z. Naturforsch., A: Phys. Sci. **2**, 615 (1947).
[32] F. Thon and D. Willasch, Mikroskopie **28**, 364 (1973).
[33] H. G. Badde and L. Reimer, Z. Naturforsch. A **25**, 760 (1970).
[34] R. Danev, R. M. Glaeser, and K. Nagayama, Ultramicroscopy **109**, 312 (2009).
[35] R. J. Hall, E. Nogales, and R. M. Glaeser, J. Struct. Biol. **174**, 468 (2011).
[36] R. Danev and K. Nagayama, Ultramicroscopy **88**, 243 (2001).
[37] F. Hosokawa, R. Danev, Y. Arai, and K. Nagayama, J. Electron Microsc. **54**, 317 (2005).
[38] R. Danev and K. Nagayama, J. Struct. Biol. **161**, 211 (2008).
[39] M. Yamaguchi, R. Danev, K. Nishiyama, K. Sugawara, and K. Nagayama, J. Struct. Biol. **162**, 271 (2008).
[40] K. Murata, X. A. Liu, R. Danev, J. Jakana, M. F. Schmid, J. King, K. Nagayama, and W. Chiu, Structure **18**, 903 (2010).
[41] K. Nagayama and R. Danev, Philos. Trans. R. Soc. London, Ser. B **363**, 2153 (2008).
[42] K. Nagayama, Eur. Biophys. J. **37**, 345 (2008).
[43] M. Marko, A. Leith, C. Hsieh, and R. Danev, J. Struct. Biol. **174**, 400 (2011).
[44] W. Ehrenberg and R. E. Siday, Proc. Phys. Soc. London, Sec. B **62**, 8 (1949).
[45] P. N. T. Unwin, J. Microsc. (Oxford) **98**, 299 (1973).
[46] W. Krakow and B. M. Siegel, Optik **42**, 245 (1975).
[47] G. Balossier and N. Bonnet, Optik **58**, 361 (1981).
[48] M. Malac, M. Beleggia, M. Kawasaki, P. Li, and R. F. Egerton, Ultramicroscopy **118**, 77 (2012).
[49] R. M. Glaeser and K. H. Downing, Microsc. Microanal. **10**, 790 (2004).
[50] K. Schultheiss, F. Perez-Willard, B. Barton, D. Gerthsen, and R. R. Schroder, Rev. Sci. Instrum. **77**, 033701 (2006).
[51] D. Alloyeau, W. K. Hsieh, E. H. Anderson, L. Hilken, G. Benner, X. Meng, F. R. Chen, and C. Kisielowski, Ultramicroscopy **110**, 563 (2010).
[52] B. Barton *et al.*, Ultramicroscopy **111**, 1696 (2011).
[53] A. Walter *et al.*, Ultramicroscopy **116**, 62 (2012).
[54] T. Tamaki, H. Kasai, K. Harada, Y. Takahashi, and R. Nishi, Microsc. Microanal. **19**, 1148 (2013).
[55] J. Shiue *et al.*, J. Electron Microsc. **58**, 137 (2009).
[56] R. Cambie, K. H. Downing, D. Typke, R. M. Glaeser, and J. Jin, Ultramicroscopy **107**, 329 (2007).
[57] H. Rose, Ultramicroscopy **110**, 488 (2010).
[58] R. R. Schroder, B. Barton, H. Rose, and G. Benner, Microsc. Microanal. **13**, 136 (2007).
[59] S. Hettler, B. Gamm, M. Dries, N. Frindt, R. R. Schroder, and D. Gerthsen, Microsc. Microanal. **18**, 1010 (2012).
[60] C. J. Edgcombe, A. Ionescu, J. C. Loudon, A. M. Blackburn, H. Kurebayashi, and C. H. W. Barnes, Ultramicroscopy **120**, 78 (2012).
[61] Y. Aharonov and D. Bohm, Phys. Rev. **115**, 485 (1959).
[62] T. H. Boyer, Found. Phys. **32**, 41 (2002).
[63] T. H. Boyer, Phys. Rev. D **8**, 1679 (1973).
[64] S. Furhapter, A. Jesacher, S. Bernet, and M. Ritsch-Marte, Opt. Express **13**, 689 (2005).
[65] J. Verbeeck, H. Tian, and P. Schattschneider, Nature (London) **467**, 301 (2010).
[66] P. Schattschneider and J. Verbeeck, Ultramicroscopy **111**, 1461 (2011).
[67] B. J. McMorran, A. Agrawal, I. M. Anderson, A. A. Herzing, H. J. Lezec, J. J. McClelland, and J. Unguris, Science **331**, 192 (2011).
[68] N. Voloch-Bloch, Y. Lereah, Y. Lilach, A. Gover, and A. Arie, Nature (London) **494**, 331 (2013).
[69] A. Jesacher, S. Furhapter, S. Bernet, and M. Ritsch-Marte, Phys. Rev. Lett. **94**, 233902 (2005).
[70] G. S. Settles, *Schlieren and Shadowgraph Techniques : Visualizing Phenomena in Transparent Media* (Springer, Berlin, 2001).

[71]B. Buijsse, F. M. H. M. van Laarhoven, A. K. Schmid, R. Cambie, S. Cabrini, J. Jin, and R. M. Glaeser, Ultramicroscopy **111**, 1688 (2011).

[72]G. B. Haydon and R. A. Lemons, J. Microsc. (Oxford) **95**, 483 (1972).

[73]A. G. Cullis and D. M. Maher, Ultramicroscopy **1**, 97 (1975).

[74]R. Danev and K. Nagayama, J. Phys. Soc. Jpn. **73**, 2718 (2004).

[75]Y. Kaneko, R. Danev, K. Nitta, and K. Nagayama, J. Electron Microsc. **54**, 79 (2005).

[76]Y. Kaneko, R. Danev, K. Nagayama, and H. Nakamoto, J. Bacteriol. **188**, 805 (2006).

[77]B. Barton, F. Joos, and R. R. Schröder, J. Struct. Biol. **164**, 210 (2008).

[78]H. Mueller, J. A. Jin, R. Danev, J. Spence, H. Padmore, and R. M. Glaeser, New J. Phys. **12**, 073011 (2010).

[79]J. F. Dawson and Z. Fried, Phys. Rev. Lett. **19**, 467 (1967).

[80]H. Okamoto, Phys. Rev. A **81**, 043807 (2010).

[81]H. Okamoto, Phys. Rev. A **85**, 043810 (2012).

[82]R. H. Rochat, X. Liu, K. Murata, K. Nagayama, F. J. Rixon, and W. Chiu, J. Virol. **85**, 1871 (2011).

[83]R. M. Glaeser *et al.*, Ultramicroscopy **135**, 6 (2013).

[84]E. Majorovits, B. Barton, K. Schultheiss, F. Perez-Willard, D. Gerthsen, and R. R. Schroder, Ultramicroscopy **107**, 213 (2007).